Journal of Experimental Botany, Vol. 63, No. 1, pp. 329–340, 2012
doi:10.1093/jxb/err276 Advance Access publication 20 September, 2011
This paper is available online free of all access charges (see http://jxb.oxfordjournals.org/open_access.html for further details)

Journal of Experimental Botany
www.jxb.oxfordjournals.org

RESEARCH PAPER

Functional associations between the metabolome and manganese tolerance in *Vigna unguiculata*

Hendrik Führs[1,*], André Specht[1], Alexander Erban[2], Joachim Kopka[2] and Walter J. Horst[1,*]

[1] Institute of Plant Nutrition, Faculty of Natural Sciences, Leibniz University Hannover, Herrenhäuser Str. 2, D-30419 Hannover, Germany
[2] Max Planck Institute of Molecular Plant Physiology, Am Mühlenberg 1, D-14476 Potsdam-Golm, Germany

* To whom correspondence should be addressed. E-mail: fuehrs@pflern.uni-hannover.de or horst@pflern.uni-hannover.de

Received 23 June 2011; Revised 4 August 2011; Accepted 5 August 2011

Abstract

Genotypic- and silicon (Si)-mediated differences in manganese (Mn) tolerance of cowpea (*Vigna unguiculata*) arise from a combination of symplastic and apoplastic traits. A detailed metabolomic inspection could help to identify functional associations between genotype- and Si-mediated Mn tolerance and metabolism. Two cowpea genotypes differing in Mn tolerance (TVu 91, Mn sensitive; TVu 1987, Mn tolerant) were subjected to differential Mn and Si treatments. Gas chromatography–mass spectrometry (GC-MS)-based metabolite profiling of leaf material was performed. Detailed evaluation of the response of metabolites was combined with gene expression and physiological analyses. After 2 d of 50 μM Mn supply TVu 91 expressed toxicity symptoms first in the form of brown spots on the second oldest trifoliate leaves. Silicon treatment suppressed symptom development in TVu 91. Despite higher concentrations of Mn in leaves of TVu 1987 compared with TVu 91, the tolerant genotype did not show symptoms. From sample cluster formation as identified by independent component analysis (ICA) of metabolite profiles it is concluded that genotypic differences accounted for the highest impact on variation in metabolite pools, followed by Mn and Si treatments in one of two experiments. Analysis of individual metabolites corroborated a comparable minor role for Mn and Si treatments in the modulation of individual metabolites. Mapping individual metabolites differing significantly between genotypes onto biosynthetic pathways and gene expression studies on the corresponding pathways suggest that genotypic Mn tolerance is a consequence of differences (i) in the apoplastic binding capacity; (ii) in the capability to maintain a high antioxidative state; and (iii) in the activity of shikimate and phenylpropanoid metabolism.

Key words: Antioxidative capacity, metabolomics, Mn chelation, shikimate and phenylpropanoid metabolism.

Introduction

Manganese (Mn) toxicity represents a major factor limiting plant growth particularly in areas of the tropics and subtropics (Horst, 1988). A considerable variation in Mn tolerance has been observed between plant species and between cultivars within a plant species (Foy *et al.*, 1978). High inter- and intraspecific variation in Mn tolerance serves as a valuable source for studies on Mn tolerance mechanisms and breeding programmes for Mn tolerance. Another tolerance factor is silicon (Si). Silicon, taken up by plants as uncharged silicic acid, has several beneficial effects on plant growth since it increases biotic and abiotic stress tolerance including Mn toxicity stress (Epstein, 1999). The physiology of Mn toxicity stress alleviation by Si in plants is currently only poorly understood even though studies report an effect of Si on apoplastic/cell wall Mn-binding properties (Iwasaki *et al.*, 2002*a*, *b*; Rogalla and Römheld, 2002). Recently, Führs *et al.* (2009) suggested that Si could reduce symptom development due to Mn toxicity by constitutive modulation of the metabolome or by modifying metabolic responses to Mn toxicity stress.

Recent studies focused on comparing the cowpea cultivars, Mn-sensitive cv. TVu 91 and Mn-tolerant cv. TVu 1987, which differ considerably in Mn tolerance. These studies were based on '-omics' approaches and suggested

that Mn toxicity stress involves a coordinated interplay of events which take place in both the apoplast and symplast. Apoplastic peroxidase (POD) activities correlate with the toxicity stress level of the plants (Fecht-Christoffers *et al.*, 2006; Führs *et al.*, 2009). A key role of apoplastic PODs in the modulation of the apoplastic redox status was suggested. Führs *et al.* (2009) found that the activity of POD isoenzymes is specifically modulated by aromatic compounds and Mn. POD isoenzymes seemed to play a role in balancing apoplastic reactive oxygen species (ROS), particularly H_2O_2. Proteomic results revealed genotypic differences in primary energy metabolism as an indirect effect of state I to state II transitions of photosynthesis (Führs *et al.*, 2008).

Investigations on other plant species focused on Mn homeostasis as a factor contributing to Mn tolerance; that is, sequestration of Mn^{2+} into biochemically inert cell compartments (Pittman, 2005). Investigations on Mn accumulation in cowpea also revealed differences in Mn compartmentation. These findings, however, were not sufficient to explain genotypic differences in Mn tolerance between genotypes (Fecht-Christoffers *et al.*, 2007).

Metabolomics in plant science was proven to be a valuable tool for phenotyping and diagnostic analysis of plants (Schauer and Fernie, 2006). This technique is used in several areas of plant science including studies on responses of legume plants to biotic and abiotic stresses (Sanchez *et al.*, 2010). Comparative metabolomics has been shown to provide new insights into non-sequenced plant systems with limited accessibility to molecular tools (e.g. Sanchez *et al.*, 2011).

In contrast to previously published results on Mn toxicity in cowpea, in this study the focus was primarily on a possible mechanistic association of metabolism and Mn tolerance. This was realized by application of a metabolic phenotyping approach using a successfully established experimental system for Mn tolerance research which includes two cowpea genotypes that exhibit considerable differences in Mn tolerance (Fecht-Christoffers *et al.*, 2006, 2007; Führs *et al.*, 2008, 2009) and experiments designed for testing for genotype, Mn, and Si interactions. This approach was then further backed up and verified by specifically designed transcriptional and physiological measurements. The aim was to identify metabolic responses and key factors associated with Mn tolerance, which can either be acquired by Si treatment or, more importantly, are constitutively present in Mn-tolerant cultivars; outcomes would facilitate focusing future research in the area of Mn tolerance.

Materials and methods

Plant material

Cowpea [*Vigna unguiculata* (L.) Walp.] genotypes TVu 91 (Mn sensitive) and TVu 1987 (Mn tolerant) were grown hydroponically in a growth chamber under controlled environmental conditions at 30/27 °C day/night temperatures, 75±5% relative humidity, and a photon flux density of 150 µmol $m^{-1}s^{-1}$ photosynthetic active radiation (PAR) at mid-plant height during a 16 h photoperiod. After germination in 1 mM $CaSO_4$ for 7 d, seedlings were transferred for pre-culture to a constantly aerated nutrient solution. The composition of the nutrient solution was (µM): $Ca(NO_3)_2$ 1000, KH_2PO_4 100, K_2SO_4 375, $MgSO_4$ 325, FeEDDHA 20, NaCl 10, H_3BO_3 8, $MnSO_4$ 0.2, $CuSO_4$ 0.2, $ZnSO_4$ 0.2, and Na_2MoO_4 0.05. The highest Mn toxicity-alleviating effect of Si in cowpea was observed when it was applied before and during excess Mn treatment (Iwasaki *et al.*, 2002*a*, *b*). Therefore, Si-treated plants received Si in the form of Aerosil© [chemically clean pyrogenic silicic acid, solubility in water 20–26.5 µM as plant-available orthosilicic acid (H_4SiO_4), in the following termed Si; Horst and Marschner (1978)] during pre-culture (+Si). After pre-culture for 14 d, the Mn concentration in the nutrient solution was increased from 0.2 µM (–Mn) to 50 µM (+Mn) for 3 d for Mn treatment, whereas control plants received 0.2 µM (–Mn) Mn continuously. During Mn treatment, Si-fed plants continuously received Si. Plants of all treatments were harvested at the same time. During the whole pre-culture and the experiment, the nutrient solution was changed 2–3 times per week to avoid nutrient deficiencies. The above-described experiment was repeated twice. In the first experiment, one plant was grown per 5.0 l pot, whereas in the second experiment the plant density in the growth chamber was increased to four plants per pot to increase the Mn toxicity stress level through modulation of the canopy light distribution at mid-plant height (Wissemeier and Horst, 1992).

Manganese analysis and quantification of toxicity symptoms

Determination of Mn in the bulk leaf tissue and quantification of Mn toxicity symptoms was done as described earlier (Führs *et al.*, 2009). Briefly, Mn in the bulk leaf tissue was determined in the second oldest middle trifoliate leaf after dry ashing at 480 °C for 8 h, dissolving the ash in 6 M HCl with 1.5% (w/v) hydroxylammonium chloride, and then diluting (1:10) with double-demineralized water. Measurements were carried out by inductively coupled plasma optical emission spectroscopy (Spectro Analytical Instruments GmbH, Kleve, Germany).

For the quantification of Mn toxicity symptoms, the density of brown spots was counted on a 1.54 cm^2 area at the base and tip on the upper side of the second oldest middle trifoliate leaf and calculated on a per cm^2 basis.

Photosynthesis rate

The photosynthesis rate was measured as described by Führs *et al.* (2008) with four replications on the second oldest middle trifoliate leaf with a Li-Cor 6400 portable photosynthesis system (LiCor Inc., Lincoln, NE, USA) using a CO_2 curve programme with the following sequence: 400, 600, 800, 1000, and 400 µmol CO_2 mol^{-1} and a flux of 500 µmol s^{-1}. Leaves received 1500 µmol PAR m^{-2} s^{-1}. The photosynthesis rate was calculated immediately by the Li-Cor control software.

GC-MS-based metabolite profiling

For gas chromatography–mass spectrometry (GC-MS) analysis, polar metabolite fractions were extracted from 60 mg ±10% (fresh weight) frozen plant material, ground to a fine powder, with MeOH/$CHCl_3$. A fraction of polar metabolites enriched for primary metabolites was prepared by liquid partitioning into water/methanol (polar fraction) and chloroform (non-polar fraction) as described previously (Führs *et al.*, 2009). In detail, metabolite samples were derivatized by methoxyamination, using a 20 mg ml^{-1} (w/v) solution of methoxyamine hydrochloride in pyridine, and subsequent trimethylsilylation, with *N*-methyl-*N*-(trimethylsilyl)-trifluoroacetamide (Fiehn *et al.*, 2000; Roessner *et al.*, 2000). A C_{12}, C_{15}, C_{19}, C_{22}, C_{28}, C_{32}, and C_{36} *n*-alkane mixture was used for the determination of retention time indices

(Strehmel *et al.*, 2008). Ribitol and deuterated alanine were added for internal standardization. Samples were analysed using GC-TOF-MS (ChromaTOF software, Pegasus driver 1.61; LECO, http://www.leco.com). GC-TOF-MS profiles of six conditions [genotype (TVu 91/TVu 1987), Mn treatment (±Mn), and Si treatment (±Si)], each with six replicates, were processed after conversion into NetCdf file format and evaluated using TagFinder software (Luedemann *et al.*, 2008). Peak height representing a mass-specific arbitrary detector response was used for the screening of relative changes of metabolite pools. The metabolite specific mass responses were normalized by leaf fresh weight and ribitol recovery. The mass spectral and retention index (RI) collection of the Golm metabolome database (Hummel *et al.*, 2010) was used for manually supervised metabolite identification. This process was supported by TagFinder (Luedemann *et al.*, 2008) and NIST08 (http://www.nist.gov/srd/mslist.htm) software. As yet unidentified metabolic components were disregarded for the current study.

Statistical analysis of GC-MS profiles

Prior to statistical data assessment, response ratios were calculated based on the mean response of each metabolic feature from all samples of the experimental data set (Führs *et al.*, 2009). These response ratios were subsequently $\log_{10}$ transformed and used for statistical and visual data analysis. Independent component analysis (ICA) and missing value substitution were as described previously (Scholz *et al.*, 2005). ICA was carried out using the first five principal components obtained from the set of manually identified metabolites. Each metabolite was represented by at least three specific and selective mass fragments. Analysis of variance (ANOVA) and statistical significance testing of pairwise comparisons (Student's *t*-test) were performed with Multi Experiment Viewer (MeV; Saeed *et al.*, 2003) and SAS statistical analysis software (SAS Institute Inc., Cary, NC, USA). ICA and three-way ANOVA were conducted independently for each experiment.

Display of the results and pathway representation

Metabolites were screened for reliable condition-dependent over-representations. These metabolites were assigned to metabolic pathways which were chosen on the basis of the number and magnitude of the observed significant metabolic changes. The pathways are the tricarboxylic acid (TCA) cycle (Fig. 4), biosynthesis of sugar alcohols (Fig. 6), and a simplified combination of the shikimate and phenylpropanoid pathway (Fig. 7). Some metabolites (e.g. sugars and organic acids not participating in the TCA cycle) are presented without reference to a pathway. Only metabolic changes which were significant in the first experiment and could be confirmed by the modified second experiment were included, but only the results of the first experiment are shown. Changes in metabolite pools are displayed as principally shown in Fig. 3; due to the predominant impact of genotypic differences on the overall experimental variation in the metabolome (see the Results), the focus was on the comparison of genotypes; they are directly compared for each Mn/Si treatment combination (from the left to the right in each graph starting with –Mn/–Si, –Mn/+Si, +Mn/–Si, and +Mn/+Si) using $\log_{10}$-response ratios. This way of displaying the data allows treatment-dependent pool size changes to be followed. Since in most cases no significant interaction effects have been observed by ANOVA, graphs of $\log_{10}$-response ratios were displayed only with *t*-test results ($^*P < 0.05$) for an easy to understand presentation of the graphs. Where needed, results of three-factorial ANOVAs are given in the graph description or in the text.

Aromatic compound analysis using HPLC

For analysis of total phenolic compounds 25–50 mg of fresh leaf material was homogenized in 1 ml of 0.5 M NaOH in a Retsch swinging mill (Retsch, Haan, Germany) at 40 Hz for 4 min. The homogenate was incubated overnight at room temperature in the dark. Afterwards the samples were acidified to pH 2 with 1 N HCl. A 100 µl aliquot of methanol was added to the samples and then topped up with water to a final volume of 2 ml. After centrifugation at 12 000 *g* for 5 min, 20 µl of supernatant was directly injected into the high-performance liquid chromatography (HPLC)system (Agilent Technologies, 1200 Series). An Eclipse XDB-C18 column (5 µm, 4.6×150 mm, Agilent Technologies) was used at a temperature of 35 °C. The mobile phase used was: (A) MeOH and (B) formic acid [5% (v/v)]. The solvent gradient changed as follows: (i) 0–32 min from 80% A/20% B to 70% A/30% B at a flow rate of 1.5 ml min^{-1}; (ii) 32–36 min from 70% A/30% to 0% A/100% B at a flow rate of 1.5 ml min^{-1}; and (iii) 36–40 min from 0% A/100% B to 80% A/20% B at a flow rate of 1.5 ml min^{-1}. Absorption was measured at 230, 266, 280, and 320 nm as well as the spectrum. Calibrations were carried out with standard solutions of *p*-hydroxybenzoic acid, *p*-coumaric acid, *o*-coumaric acid, ferulic acid, caffeic acid, and benzoic acid (Sigma-Aldrich Chemie GmbH, Munich, Germany). Results were calculated on a fresh weight basis.

RNA extraction from leaves and quantitative real-time PCR (qRT-PCR)

In order to support the metabolomic findings, a systematic expression analysis of genes involved in different metabolism pathways was performed. The expressed sequence tag (EST) database Harvest: Cowpea (http://www.harvest-web.org/) served as a source for primer design. Detailed information on the EST database accession numbers and primer sequences are given as supporting information (Supplementary Table S1 available at *JXB* online). RNA extraction was again from the second oldest fully developed leaf using Trisure© reagent (Bioline GmbH, Luckenwalde, Germany) according to the manufacturer's instructions. Sample preparation, primer efficiency testing, and final qRT-PCR were done as described previously (Eticha *et al.*, 2010).

Statistical analysis of Mn and Si concentrations and apoplastic enzyme activities

Statistical analysis, if not stated otherwise, was carried out using SAS Release v8.0 (SAS Institute). Results from ANOVA are given according to their level of significance as ***, **, and * for $P < 0.001$, 0.01, and 0.05, respectively. Pairwise comparisons were performed using Student's *t*-test.

Results

Mn toxicity

In the first experiment, elevated Mn supply for 3 d resulted in a consistent increase in the bulk-leaf Mn concentration in both cultivars (Fig. 1) with significantly higher Mn concentrations in Mn-tolerant cv. TVu 1987, as was demonstrated by a significant Mn×genotype interaction ($P < 0.001$). Si treatment did not decrease but significantly enhanced Mn tissue concentrations in both the Mn-tolerant and the Mn-sensitive cultivar (significant Si effect according to ANOVA). The first brown spots appeared on the old leaves only in Mn-sensitive cv. TVu 91 after 2 d of elevated Mn treatment and reached 10–15 brown spots cm^{-2} (moderate Mn toxicity) after 3 days.

Manganese uptake and symptom development of the second experiment were principally as described in a previous study with similar experimental conditions (Führs *et al.*, 2009). Briefly, Si did not affect Mn uptake but

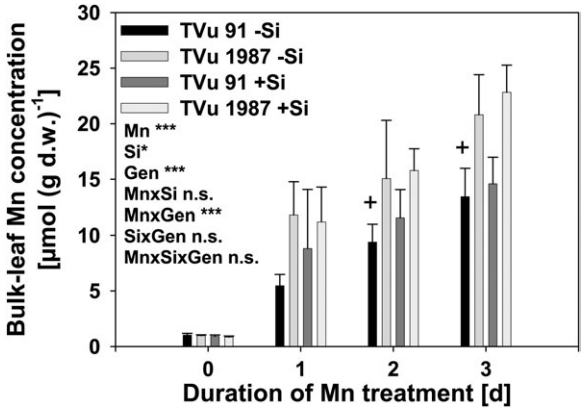

Fig. 1. Effect of duration of Mn treatment and Si supply on Mn tissue concentrations and expression of toxicity symptoms in the second oldest trifoliate leaves of the Mn-sensitive cowpea cultivar TVu 91 and the Mn-tolerant cultivar TVu 1987 in the first experiment. After 2 weeks of pre-culture at optimum 0.2 µM Mn (–Mn), the Mn supply was increased to 50 µM (+Mn) for 3 d, whereas control plants received 0.2 µM Mn continuously. Silicon treatments (+Si) received Aerosil© throughout plant culture and the experiments (see the Materials and methods). Plus signs indicate the appearance of toxicity symptoms (10–15 brown spots cm^{-2}) on leaves of the Mn-sensitive cultivar. The inset shows the results of the ANOVA for significant main and interacting effects, n.s. non-significant, ***, * for P <0.001 and 0.05, respectively.

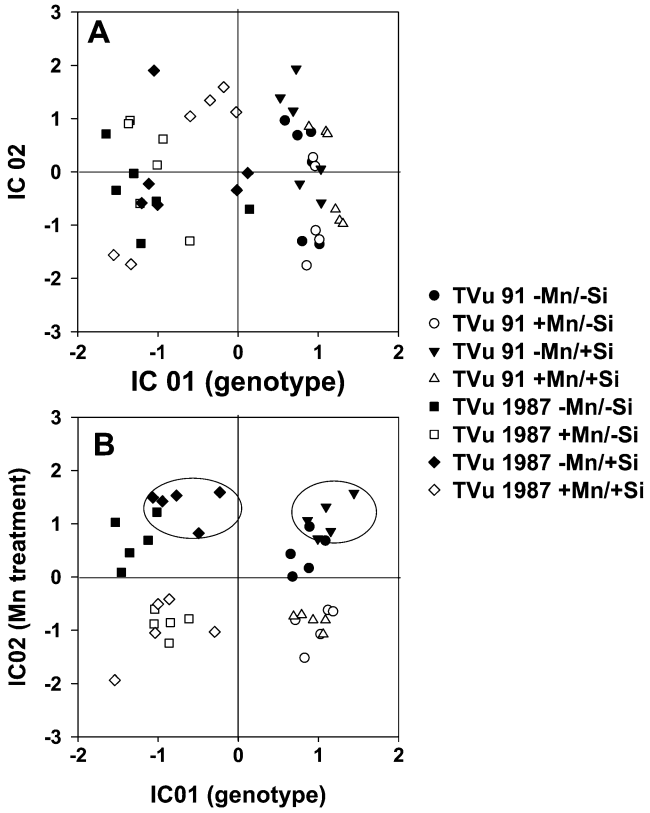

Fig. 2. ICA plot of the GC-MS-accessible bulk leaf metabolome derived from two different experiments (A, B), each with 5–6 replications. The second oldest trifoliate leaf of the Mn-sensitive cultivar TVu 91 and the Mn-tolerant cultivar TVu 1987 were tested for Mn and Si effects. After 2 weeks of pre-culture at optimum 0.2 µM Mn, the Mn supply was increased to 50 µM (+Mn) for 3 d, whereas control plants received 0.2 µM Mn (–Mn) continuously. Silicon treatments (+Si) received Aerosil© throughout plant culture and the experiments (see the Materials and methods). Leaf metabolites were extracted as described in the Materials and methods. ICA was conducted using MetaGeneAlyse at http://metagenealyse.mpimp-golm.mpg.de. IC: independent component. If apparent, the dominating experimental factor of an IC is indicated in parentheses after the IC depiction. Experiment B was performed under modified canopy light distribution conditions that were introduced to increase the Mn toxicity stress level slightly at a given Mn treatment (50 µM) duration (see the Materials and methods).

significantly delayed symptom development (data not shown). At higher plant densities of the second experiment plants developed up to 45–60 brown spots cm^{-2} leaf area, which can be regarded as medium–severe symptom expression.

Global metabolic trends

ICA allows investigation of sample clusters formed by major variances due to treatment-dependent quantitative and qualitative changes in metabolite pools. According to ICA, in the first experiment samples clustered only according to the genotypes, but neither Mn nor Si treatments appeared to have a major effect on the metabolome (Fig. 2A). Under modified canopy light distribution and, therefore, a higher Mn toxicity stress level of the second experiment, the first and most important independent component reproduced the genotype (IC01, independent component 01) effect, indicating a robust and reliable constitutive difference in the metabolome between the genotypes. The Mn treatment also contributed to cluster formation of samples (IC02; Fig. 2B). In addition, sample clusters according to Si treatment became visible among Mn control plants (samples treated with Si are indicated by black rings in Fig. 2B).

Genotypic differences in metabolite pools and their modulation by excess Mn and Si supply

The glucose-6-phosphate pool differed between the genotypes, with a larger pool in the Mn-sensitive cv. TVu 91 (Fig. 3A). In the same genotype, the glucose-6-phosphate pool decreased under Si, Mn, and combined Mn and Si treatments, whereas the opposite is true for the Mn-tolerant genotype. The Mn-tolerant cv. TVu 1987 shows invariant fructose and glucose levels (Fig. 3B, C). Under unstressed (–Mn/–Si, –Mn/+Si) conditions, the Mn-sensitive cv. TVu 91 showed small glucose and fructose pools, but had increased metabolite levels under Mn toxicity stress treatment. Si treatment affected neither glucose nor fructose pools in both cultivars.

Some of the detected organic acids form part of the TCA cycle, which is displayed in Fig. 4. Some identified organic acids (particularly α-ketoglutaric acid, succinic acid, and

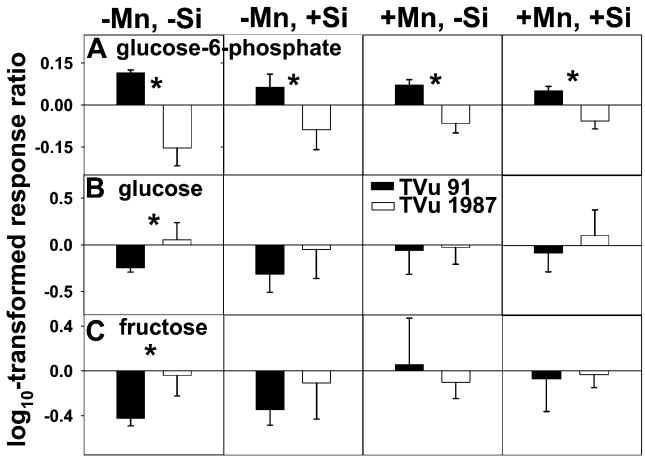

Fig. 3. Comparison of (A) glucose-6-phosphate, (B) glucose, and (C) fructose concentrations between the Mn-sensitive cowpea cultivar TVu 91 and the Mn-tolerant cultivar TVu 1987. Within each graph the genotypes are directly compared for each Mn/Si treatment combination (from the left to the right in each graph starting with –Mn/–Si, –Mn/+Si, +Mn/–Si, and +Mn/+Si) using $\log_{10}$-response ratios (see 'Statistical analysis of GC-MS profiles'). The treatments were 0.2 μM Mn for –Mn, 50 μM Mn for +Mn, 0 μM Si for –Si, and 20 μM Si for +Si. Asterisks indicate significant differences between the genotypes according to Tukey test.

malic acid) were higher in Mn-treated plants of the Mn-sensitive cv. TVu 91 than in the Mn-tolerant cv. TVu 1987 independent of the Si supply. Treatment-dependent effects within genotypes were not significant. Subsequent qRT-PCR analyses of genes coding for enzymes involved in the TCA cycle (aconitase, pyruvate dehydrogenase, isocitrate dehydrogenase, succinyl-CoA ligase, fumarase, and malate dehydrogenase) showed neither constitutive genotypic nor excess Mn-induced and Si treatment effects at the transcriptional level (Supplementary Fig. S1 at *JXB* online).

Loadings derived from unsupervised ICA indicated aspartic and glutamic acid to be mainly responsible for genotypic cluster formation (data not shown) due to their small pools. Both amino acids were invariant throughout treatments, and did not differ between both cultivars (Supplementary Fig. S2 at *JXB* online). Screening for other amino acids revealed that in non-stressed (–Mn/–Si, –Mn/+Si, and +Mn/+Si) plants of the Mn-sensitive cv. TVu 91 the pools of alanine, serine, threonine, and phenylalanine were significantly smaller than in the Mn-tolerant cv. TVu 1987. This significant genotypic difference disappeared under conditions of Mn toxicity stress (+Mn/–Si) due to an increase in amino acid pools in the Mn-sensitive cv. TVu 91. Moreover, for phenylalanine, ANOVA revealed a significant Mn and Mn×genotype interaction owing to a significant increase due to Mn treatment (see also the following sections and Supplementary Fig. S2). In principle, asparagine followed the same pattern observed for the other amino acids, but the differences observed were not significant.

The ICA procedure showed that tartaric acid significantly affected genotypic cluster formation (data not shown). ANOVA and *t*-test results confirmed that tartaric acid was indeed much higher in the Mn-tolerant cv. TVu 1987 than in the Mn-sensitive cv. TVu 91 independent of treatment (Fig. 5A). In contrast, but less pronounced, malonic acid was present in higher concentrations in the Mn-sensitive cv. TVu 91 regardless of Mn and Si treatments (Fig. 5B). Si supply increased malonic acid abundance in this cultivar. Also, quinic acid strongly affected sample cluster formation in both experiments (loadings not shown). Statistical analyses showed that it was constitutively more highly abundant in the Mn-tolerant cv. TVu 1987 (Fig. 5C), making quinic acid a candidate metabolite for further studies. Quinic acid and its derivatives play roles in synthesis of both aromatic amino acids and phenylpropanoids, and consequently cell wall composition. To follow both main pathways, the expression of a gene coding for *p*-coumaryl-CoA:quinate hydroxycinnamoyltransferase (HCT) was checked. This enzyme utilizes quinate to form *p*-coumaryl quinate (Hoffmann *et al.*, 2003). Expression studies with *HCT* showed lower expression in the Mn-tolerant cv. TVu 1987 than in the Mn-sensitive cv. TVu 91 correlating with higher quinic acid concentrations particularly under Mn, Si, and combined treatment (Fig. 5D). Quinic acid could also enter the shikimate pathway by quinate/shikimate dehydrogenase activity which forms part of the shikimate pathway. Unfortunately, there was no apparent orthologue of the quinate/shikimate dehydrogenase gene in the EST database to check further whether quinic acid concentrations correlate with the expression of this gene. However, instead the expression profile of the gene coding for dehydroquinate synthase was investigated under different Mn and Si treatments. In the shikimate pathway, this enzyme uses 3-deoxy-D-arabino-heptulosonate-7-phosphate (DAHP) to form the quinic acid derivate 3-dehydroquinate. There were neither genotypic differences nor Mn-or Si-induced changes in gene expression in both cultivars (Fig. 5E).

Myo-inositol, galactinol, and raffinose concentrations were higher in the Mn-tolerant cv. TVu 1987 than in TVu 91 independent of the Mn treatment. All three sugar alcohols were placed into one pathway (Fig. 6). Ononitol, which is directly formed from *myo*-inositol by a *myo*-inositol *O*-methyltransferase (IMT) (Sheveleva *et al.*, 1997), was higher in TVu 91 than in TVu 1987. ANOVA did not show effects of Mn and Si treatments on the abundance of these metabolites. Since the EST database did not provide any sequence information on putative *IMT* genes, no expression analysis was performed, but gene expression analysis of galactinol synthase and raffinose synthase genes was possible (given in the inlay graph of Fig. 6 as A, B). Expression analyses of both genes corroborated the metabolome findings. Particularly under non-stressed (–Mn/–Si, –Mn/+Si, and +Mn/+Si) conditions both genes were more highly expressed in the Mn-tolerant cv. TVu 1987 than in TVu 91. The raffinose synthase gene showed equal expression between Mn-treated plants of both genotypes.

A combination of the shikimate and phenylpropanoid pathway is shown in Fig. 7. The displayed pathway starts with shikimic acid of the shikimate pathway yielding

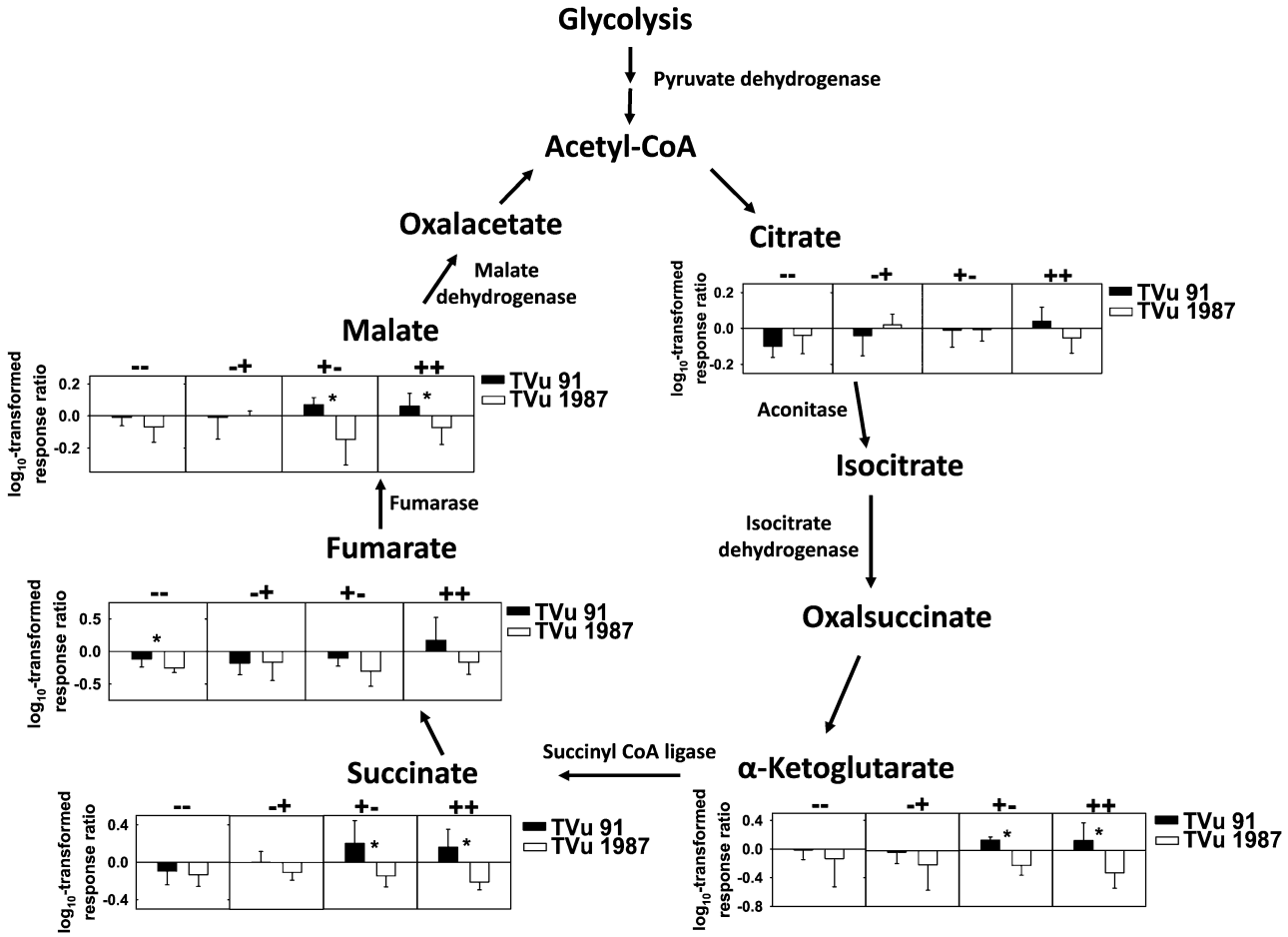

Fig. 4. TCA cycle overview. Treatment-dependent changes in the detected organic acid pools are shown in the scheme. Within each graph the Mn-sensitive cowpea cultivar TVu 91 and the Mn-tolerant cultivar TVu 1987 are directly compared for each Mn/Si treatment combination (from the left to the right in each graph starting with –Mn/–Si, –Mn/+Si, +Mn/–Si, and +Mn/+Si) using $\log_{10}$-response ratios (see 'Statistical analysis of GC-MS profiles'). The treatments were 0.2 μM Mn for –Mn, 50 μM Mn for +Mn, 0 μM Si for –Si, and 20 μM Si for +Si. Asterisks indicate significant differences between the genotypes according to Tukey test. Expression studies were made of genes encoding the enzymes displayed in the TCA cycle scheme (Supplementary Fig. S1 at *JXB* online).

aromatic amino acids. Under non-stressed conditions (–Mn/–Si, –Mn/+Si, and +Mn/+Si), shikimic acid and phenylalanine were higher in the Mn-tolerant TVu 1987 compared with TVu 91. In Mn-treated plants, the abundance of both metabolites was similar between genotypes due to an increased abundance in the Mn-sensitive cv. TVu 91. For phenylalanine but not for shikimic acid, the Mn effect was reflected by a significant Mn and Mn×genotype interaction. The *p*-coumaric acid pool (the only detected phenylpropanoid of the first metabolite profiling experiment) remained unaffected by either treatment and was not significantly different between the genotypes.

A HPLC analysis specifically targeting aromatic compounds was developed in order to confirm and extend GC-MS-based profiling results on aromatic compounds. Two phenylpropanoids could be identified, *p*-coumaric acid and ferulic acid (Supplementary Fig. S3 at *JXB* online). Neither compound showed Mn or Si treatment-dependent responses in either genotype, confirming the GC-MS-derived results. *p*-Coumaric acid was ~10-fold more highly abundant than ferulic acid in both cultivars, and both phenolic compounds were significantly higher in the Mn-sensitive cv. TVu 91 than in TVu 1987. Expression analysis of genes involved in the branching point between primary and secondary metabolism [the phenylalanine ammonia-lyase (*PAL*) gene] and the first steps of *p*-coumaric and ferulic acid biosynthesis [cinnamate 4-hydroxylase (*C4H*) and caffeic acid *O*-methyltransferase (*COMT*)] showed higher expression in TVu 91 compared with TVu 1987 under control conditions, whereas the expression of the 4-coumarate-CoA-ligase gene (*4CL*), which forms *p*-coumaryl-CoA, was more highly expressed in the Mn-tolerant cv. TVu 1987 (Supplementary Fig. S4 at *JXB* online). For all tested genes, the greatest difference between the genotypes occurred when Mn-treated plants were compared. In all cases the expression was higher in the sensitive cultivar. Si treatment did not affect the expression of any of the genes compared with control treatment. The expression of *PAL* and *C4H* in +Mn/+Si-treated plants was similar between the genotypes, whereas *PAL* and *COMT* were more highly expressed in +Mn/+Si treatments of the Mn-sensitive cv. TVu 91 compared with TVu 1987.

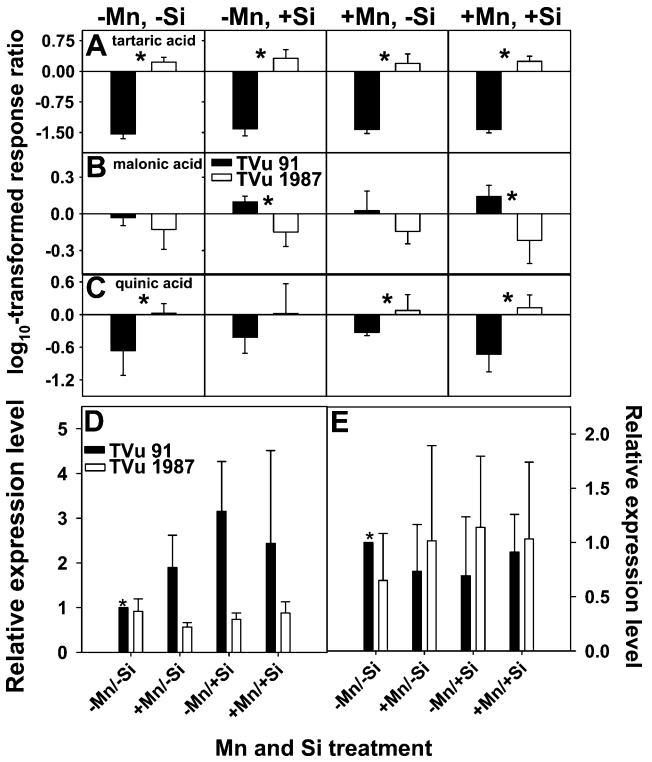

Fig. 5. (A–C) Comparison of the concentrations of (A) tartaric acid, (B) malonic acid, and (C) quinic acid between the Mn-sensitive cowpea cultivar TVu 91 and the Mn-tolerant cultivar TVu 1987. Within each graph the genotypes are directly compared for each Mn/Si treatment combination (from left to right –Mn/–Si, –Mn/+Si, +Mn/–Si, and +Mn/+Si) using $\log_{10}$-response ratios (for information on calculation of response ratios see 'Statistical analysis of GC-MS profiles'). The treatments were 0.2 μM Mn for –Mn, 50 μM Mn for +Mn, 0 μM Si for –Si, and 20 μM Si for +Si. Asterisks indicate significant differences between the genotypes according to Tukey test. (D and E) Expression analysis of ESTs with homology to (D) *p*-coumaryl-CoA:quinate hydroxycinnamoyltransferase and (E) 3-dehydroquinate synthase by means of qPT-PCR. Both enzymes are in the broadest sense involved in phenylpropanoid and cell wall composition. Sequences were derived from HarvEST: Cowpea database. RNA extraction from leaves of both cultivars and qRT-PCR were performed as described in the Materials and methods. An asterisk indicates that TVu 91 –Mn/–Si served as the calibrator for relative gene expression.

Discussion

Global Mn- and Si-induced metabolomic changes

The differences in sample clustering between the first and second experiment may be a consequence of different toxicity stress levels applied in the experiments through modified light distribution pattern/plant density (see the Materials and methods), since shading aggravates toxicity symptom development in cowpea (Wissemeier and Horst, 1992). Indeed, in the first experiment, the Mn-sensitive cv. TVu 91 exhibited 10–15 brown spots cm^{-2} leaf area typical for light to medium Mn toxicity expression. At higher plant densities, up to 50–60 brown spots cm^{-2} leaf area were counted at a comparable treatment duration which can be regarded as medium–severe symptom expression (Fecht-Christoffers *et al.*, 2003). Therefore, the toxicity stress inflicted on plants in the first experiment was too low for creation of metabolic sample clustering. In view of the ICA results, the presented changes in the metabolome of both experiments, but particularly the first experiment, can be regarded as early effects directly linked to Mn excess rather than as secondary effects induced by Mn toxicity-enhanced leaf senescence as supposed by Fecht-Christoffers *et al.* (2006, 2007).

In the second experiment, in Mn control but not in plants treated with Mn excess, Si also led to sample clusters in both cultivars, verifying results published only for the Mn-sensitive genotype TVu 91 (Führs *et al.*, 2009). It has to be stated here that cowpea as a legume belongs to the group of plants showing low ability to accumulate Si in the leaf tissue compared with Si-accumulating plant species (Epstein, 1999). Despite this low uptake characteristic, Si is obviously responsible for constitutive changes in metabolite pools, even though the impact is small compared with the other experimental factors. It remains unclear whether this Si effect is a primary or secondary effect, since the metabolomic approach used could not identify straightforward metabolic associations with Si supply. However, the influence of constitutive Si may indeed be a secondary effect probably caused by its positive impact on the 'unfavourable' (in terms of light perception) growth conditions compared with the first experiment. Unspecific positive effects of Si on plant performance were already reported for other plants species (for a review, see Epstein, 1999). However, reports on the influence of Si on biotic stress repeatedly stated that measurable effects of Si on plant metabolism typically occur when supplied together with a biotic stressor (Fauteux *et al.*, 2006; Chain *et al.*, 2009). Instead, in the present study, more pronounced Mn toxicity stress led to disappearance of the Si effect in Mn-treated plants (Fig. 2B). This shows that, under certain conditions, Si can constitutively influence the metabolome of both genotypes, which is then overlaid by enhanced Mn toxicity stress effects on the metabolism. Due to the predominant genotypic impact on the variation of both experiments compared with the effects of Mn and Si treatments, these genotypic factors are discussed in the following sections. Also, despite the identification of a number of metabolites showing significant Mn×genotype and/or Si×genotype interactions in the first experiment, these interactions could not be reproduced or unequivocally interpreted owing to significant Mn×Si×genotype interactions. Therefore, the results are not presented and are not discussed.

Mn toxicity stress creates increased energy demands and rebalancing of carbon skeletons

There are genotypic differences in hexose and hexose phosphate pools, but in particular the Mn toxicity stress-induced increase in glucose and fructose pools in the Mn-sensitive cv. TVu 91 but not in TVu 1987 indicates sensitivity-associated responses in sugar pools. The same is

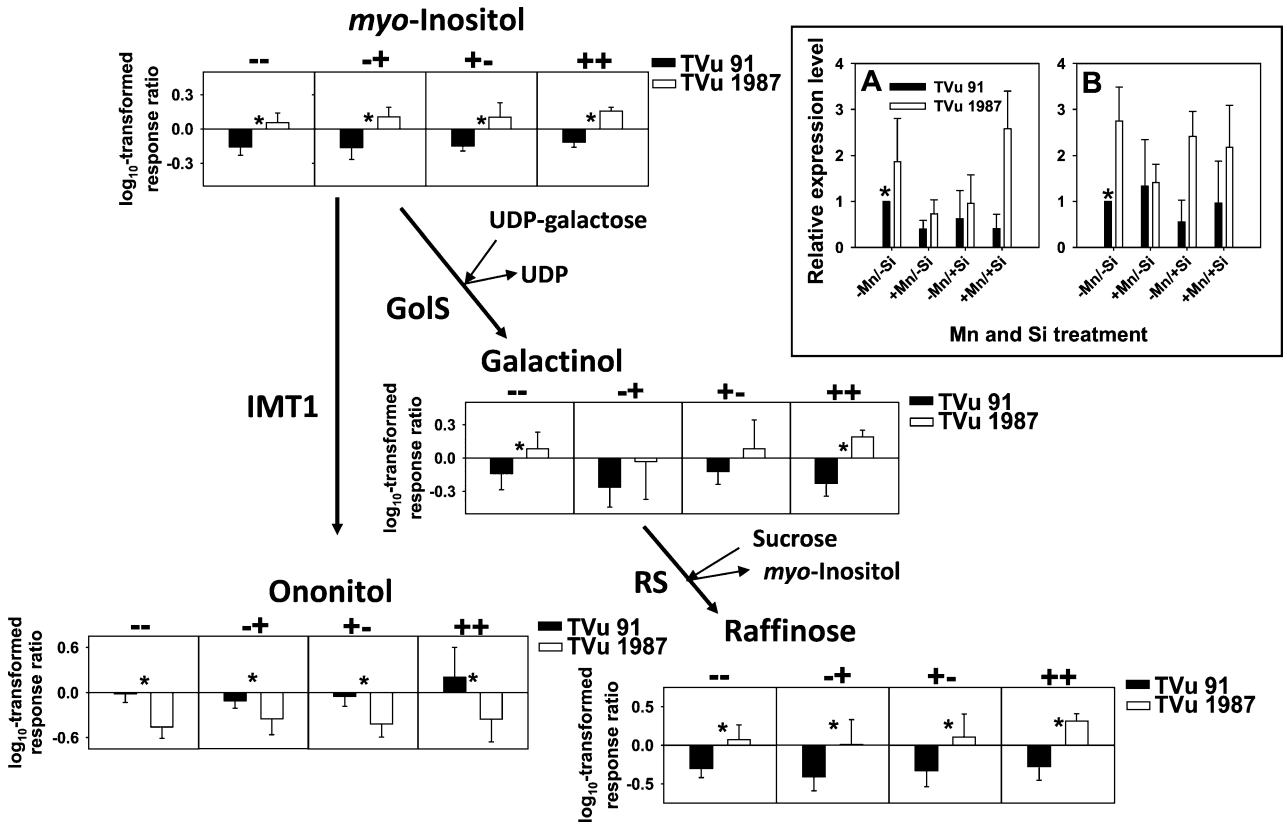

Fig. 6. Sugar alcohol pathway: partial overview. Treatment-dependent changes in the detected sugar alcohol pools are included in the scheme. Within each graph, the Mn-sensitive cowpea cultivar TVu 91 and the Mn-tolerant cultivar TVu 1987 are directly compared for each Mn/Si treatment combination (from left to right –Mn/–Si, –Mn/+Si, +Mn/–Si, and +Mn/+Si) using $\log_{10}$-response ratios (for information on calculation of response ratios see 'Statistical analysis of GC-MS profiles'). The treatments were 0.2 μM Mn for –Mn, 50 μM Mn for +Mn, 0 μM Si for –Si, and 20 μM Si for +Si. Asterisks indicate significant differences between the genotypes according to Tukey test. An expression analysis of ESTs with homology for genes encoding (A) galactinol synthase and (B) raffinose synthase was done (see inlay graph). Both genes are involved in the biosynthesis of sugar alcohols. Sequences were derived from HarvEST: Cowpea database. RNA extraction from leaves of the Mn-sensitive cowpea cultivar TVu 91 and the Mn-tolerant cultivar TVu 1987 and qRT-PCR were performed as described in the Materials and methods. An asterisk indicates that TVu 91 –Mn/–Si served as the calibrator for relative gene expression. IMT, *myo*-inositol *O*-methyltransferase; GolS, galactinol synthase; RS, raffinose synthase.

true for increased organic acid pools related to the TCA cycle and downstream associated amino acid pools in the Mn-sensitive cultivar under Mn toxicity stress conditions. Hexose phosphates form the starting point of sugar degradation for energy provision through the TCA cycle. Mn toxicity stress-enhanced abundances of hexoses in combination with an unchanged hexose phosphate pool must be realized either by increased photosynthesis rates or by sugar supply from other plant organs. To determine whether photosynthesis is responsible for increased sugar contents, net photosynthesis CO_2 response curves were measured (Supplementary Fig. S5 at *JXB* online). ANOVA performed for each individual day of Mn treatment and CO_2 supply revealed a significantly higher net carbon exchange rate in the Mn-tolerant cv. TVu 1987. No Mn toxicity stress-related modulations in carbon fixation have been observed (Supplementary Fig. S5), even though detrimental effects of excess Mn on photosynthesis have been described in other plant species (Nable *et al.*, 1988). This suggests that increased hexose pools in Mn toxicity-stressed tissues under unchanged photosynthesis rates may be a consequence of sucrose degradation, which represents the main transport form of sugars within plants, and they may be transported from physiologically younger unstressed to older stressed plant tissues.

Earlier studies proposed that changed energy demands under Mn toxicity stress could be satisfied by a higher level of state I–state II transitions of photosynthesis in Mn toxicity-stressed plants leading to cyclic electron transport and ATP production (Führs *et al.*, 2008, and references therein). In view of the new results on the TCA cycle activity, the specific role of state transitions in Mn toxicity stress responses may be reduced to electron flow balancing through the photosystems (Kruse, 2001). This is corroborated by physiological and proteomic results pointing to changed electron transport rates and genotype-specific subunit modifications of the water-splitting complex after excess Mn supply (Führs *et al.*, 2008). The observed photosynthetic modifications could be part of a photosynthesis maintenance/repair process rather than of an increased energy-providing process. Even though Walther *et al.* (2010) explicitly pointed

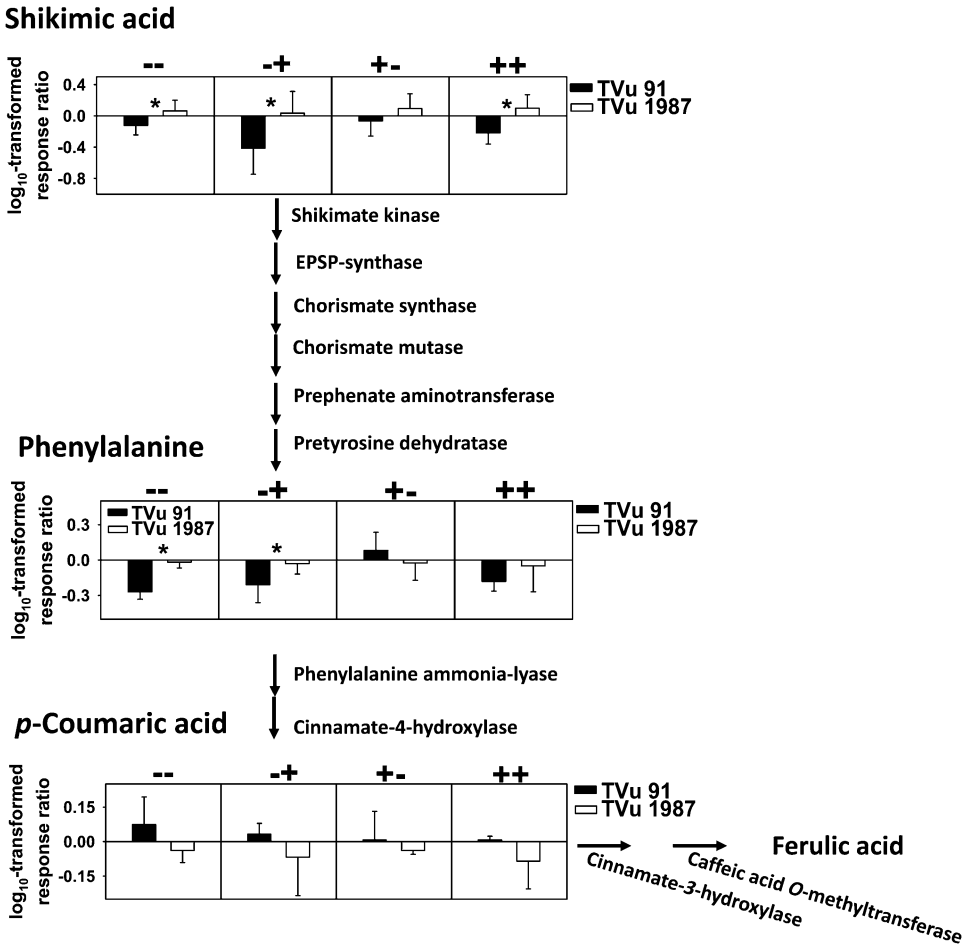

Fig. 7. Simplified combined biosynthesis pathway of hydroxycinnamic acids with *p*-coumaric acid as the primary product. Treatment-dependent changes in the detected aromatic compound pools are included in the scheme. Within each graph the Mn-sensitive cowpea cultivar TVu 91 and the Mn-tolerant cultivar TVu 1987 are directly compared for each Mn/Si treatment combination (from left to right –Mn/–Si, –Mn/+Si, +Mn/–Si, and +Mn/+Si) using $\log_{10}$-response ratios (for information on calculation of response ratios see 'Statistical analysis of GC-MS profiles'). The treatments were 0.2 μM Mn for –Mn, 50 μM Mn for +Mn, 0 μM Si for –Si, and 20 μM Si for +Si. Asterisks indicate significant differences between the genotypes according to Tukey test. The expression of ESTs with homology to phenylalanine ammonia lyase, cinnamate-4-hydroxylase, and caffeic acid *O*-methylatransferase genes (as well as that for 4-coumarate CoA ligase, not displayed here) was analysed (Supplementary Fig. S4 at *JXB* online).

out that it is dangerous to draw conclusions on metabolite fluxes just on the basis of steady-state results, it is assumed that increased energy demands are assured by increased respiration rates in mitochondria. However, transcript levels of TCA cycle-related genes did not correlate with the abundance of metabolites affected by the encoded protein. In fact, the activities of enzymes participating in the TCA cycle may have had stronger impacts on steady-state metabolite levels (Fernie *et al.*, 2005) rather than transcript levels of the corresponding gene.

Manganese tolerance is a consequence of constitutive higher concentrations of metabolites detoxifying manganese and reactive oxygen species

Fecht-Christoffers *et al.* (2007) developed a reaction scheme in which PODs play a central role in the development of toxicity symptoms. In this scheme, Mn^{II} is required as a cofactor for H_2O_2-producing POD activity. During this process, Mn^{III} is formed, a short-lived and deleterious Mn species causing lipid peroxidation. Maier (1997) concluded that formation of Mn^{II}–organic acid complexes could not explain Mn tolerance in cowpea. In this study, tartaric and malonic acid considerably differed between both cultivars without a significant treatment effect. Both tartaric acid (Podgornik *et al.*, 2001) and malonic acid (Wariishi *et al.*, 1992) are known as Mn^{III} chelators. Scavenging of Mn^{III} by complexation would terminate the recycling of Mn^{II} and remove an essential reaction intermediate for H_2O_2-producing POD activity, thus preventing oxidative stress. However, Mn^{III}–organic acid complexes themselves can act as strong oxidants (Podgornik *et al.*, 2001). Additional oxidant activity could then accelerate development of Mn toxicity. Since higher tissue concentration of both organic acids was associated with tolerance, it is suggested that formation of organic acid–Mn^{III} complexes confers Mn

tolerance in cowpea. Further studies on the Mn^{II}- and Mn^{III}-chelating power of the identified organic acids and their effect on POD activity are necessary.

Myo-inositol, galactinol, and raffinose pools were higher in the bulk leaf of TVu 1987, which correlated with higher expression of their respective genes, indicating increased sugar alcohol biosynthesis. Galactinol and raffinose were shown to function as antioxidants in plant cells (Nishizawa *et al.*, 2008). Considering the detrimental effect of excess Mn on the photosynthetic apparatus (see above) and enhanced ROS production in the apoplast (Fecht-Christoffers *et al.*, 2007; Führs *et al.*, 2009) a higher abundance of ROS-scavenging sugar alcohols in TVu 1987 would act as an Mn tolerance factor. The specific role of ononitol, which was found at higher levels in the Mn-sensitive cv. TVu 91, remains unclear. Sheveleva *et al.* (1997) reported increased salt and drought tolerance in transgenic tobacco (over-) expressing *IMT1*. Obviously, in contrast to TVu 1987, the Mn-sensitive cultivar preferably activates the pathway leading to formation of ononitol.

The decisive role of apoplastic phenols, especially ferulic and *p*-coumaric acid, in the modulation of peroxidase activity and Mn toxicity development in cowpea has been extensively described previously (Fecht-Christoffers *et al.*, 2006, 2007; Führs *et al.*, 2009). Also evidence of substantial alteration of the apoplastic phenolic compound profile in quality and quantity under Mn toxicity stress conditions has been provided previously (Fecht-Christoffers *et al.*, 2006; Führs *et al.*, 2009). Secretion of phenols into the apoplast requires biosynthesis in the symplast. Indeed, lower metabolite pools related to the shikimate pathway and higher metabolite pools of the phenylpropanoid pathway in the bulk leaf indicate a constitutive higher activity of aromatic compound metabolism in the Mn-sensitive cv. TVu 91. Moreover, under stress conditions, the expression of all checked genes of the phenylpropanoid pathway was synergistically further enhanced in the Mn-sensitive but not the Mn-tolerant cultivar. An increased synthesis of phenylpropanoids due to Mn toxicity stress may then facilitate their secretion into the apoplast. The Mn toxicity stress-enhanced activation of phenylpropanoid metabolism in the Mn-sensitive cv. TVu 91 was accompanied by increased pool sizes of members of the shikimate pathway. The shikimate pathway is typically described as a linker of carbohydrate metabolism and biosynthesis of aromatic compounds (Herrmann and Weaver, 1999). The role of increases in hexose pools as a mechanism for providing energy for energy-demanding stress responses (see above) may be extended to feeding the shikimate and, therefore, the phenylpropanoid pathway.

The quinic acid pool was constitutively higher in the Mn-tolerant cv. TVu 1987. Quinate is used by HCT (Hoffmann *et al.*, 2003). Silencing *HCT* led to quantitative and qualitative changes in the soluble phenylpropanoid pool but also in the lignin content (Hoffmann *et al.*, 2004). *HCT* expression studies showed a lower expression in the tolerant cultivar particularly under all three different treatments (+Mn; +Si; and +Mn, +Si) which correlates with higher quinic acid contents (Fig. 5C, D). This not only substantiates the already proposed (see above) Mn tolerance-specific difference in aromatic compound metabolism between the cultivars, but may also point to genotypic differences in cell wall composition. On the other hand a direct effect of Si on the expression of *HCT* in plants of the Mn-sensitive cultivar TVu 91 but not TVu 1987 has been found. One can only speculate about the reason and consequences of this Si-specific increase in lignin formation in the sensitive cultivar. Since cell wall binding properties have been shown to play a major role in Si-enhanced Mn tolerance in cucumber (Rogalla and Römheldt, 2002) and cowpea (Iwasaki *et al.*, 2002*a*, *b*) and were held responsible for the extraordinary high Mn tolerance of rice (Führs *et al.*, 2010), constitutive and Si-enhanced differences in lignin content and quality due to differences in *HCT* expression appear to be a promising starting point for future studies.

In conclusion, a search for metabolic responses and key factors associated with Mn tolerance revealed that the predominant experimental factor leading to metabolic variation is the genotype. Consequently, most associations between metabolism and Mn tolerance were identified by genotypic comparisons, for example under Mn toxicity stress. These associations suggest (i) differences in cell wall composition and binding capacity; (ii) a higher antioxidative capacity through higher abundance of specific sugar alcohols and Mn^{III}-chelating compounds; and (iii) a less active phenylpropanoid metabolism contributing to genotypic Mn tolerance. Hence, the study provides a number of physiological starting points and several candidate genes which will be subject to future studies focusing on the functional clarification of the physiological and molecular basis of genotypic differences in Mn tolerance. However, the observed physiological differences associated with Mn tolerance appear valid for cowpea, but other plant species might differ in their response to excess Mn and Si supply.

Supplementary data

Supplementary data are available at *JXB* online.

Figure S1. Expression analysis of TCA cycle-related genes.

Figure S2. Genotypic comparison of detected amino acids.

Figure S3. Genotypic comparison of bulk leaf ferulic acid and *p*-coumaric acid concentrations.

Figure S4. Expression analysis of genes involved in phenylpropanoid metabolism.

Figure S5. Genotypic comparison of CO_2 response curves after excess Mn treatment for 1–3 d.

Table S1. Primer specifications for gene expression analyses using qRT-PCR analyses.

References

Chain F, Côté-Beaulieu C, Belzile F, Menzies JG, Bélanger RR 2009. A comprehensive transcriptomic analysis of the effect of silicon

on wheat plants under control and pathogen stress conditions. *Molecular Plant-Microbe Interactions* **22,** 1323–1330.

Eticha D, Zahn M, Bremer M, Yang Z, Rangel AF, Rao IM, Horst WJ 2010. Transcriptomic analysis reveals differential gene expression in response to aluminium in common bean (*Phaseolus vulgaris*) genotypes. *Annals of Botany* **105,** 1119–1128.

Epstein E 1999. Silicon. *Annual Review of Plant Physiology and Plant Molecular Biology* **50,** 641–664.

Fauteux F, Chain F, Belzile F, Menzies JG, Bélanger RR 2006. The protective role of silicon in the Arabidopsis–powdery mildew pathosystem. *Proceedings of the National Academy of Sciences, USA* **103,** 17554–17559.

Fecht-Christoffers MM, Braun H-P, Lemaitre-Guillier C, Van Dorsselaer A, Horst WJ 2003. Effect of manganese toxicity on the proteome of the leaf apoplast in cowpea. *Plant Physiology* **133,** 1935–1946.

Fecht-Christoffers MM, Führs H, Braun H-P, Horst WJ 2006. The role of hydrogen peroxide-producing and hydrogen peroxide-consuming peroxidases in the leaf apoplast of cowpea in manganese tolerance. *Plant Physiology* **140,** 1451–1463.

Fecht-Christoffers MM, Maier P, Iwasaki K, Braun H-P, Horst WJ. 2007. The role of the leaf apoplast in manganese toxicity and tolerance in cowpea (Vigna unguiculata L. Walp). In: Sattelmacher B, Horst WJ, eds. *The apoplast of higher plants: compartment of storage, transport, and reactions*. Dordrecht: Springer, 307–322.

Fernie AR, Geigenberger P, Stitt M 2005. Flux an improtant, but neglected, component of functional genomics. *Current Opinon in Plant Biology* **8,** 174–182.

Fiehn O, Kopka J, Trethewey RN, Willmitzer L 2000. Identification of uncommon plant metabolites based on calculation of elemental compositions using gas chromatography and quadrupole mass spectrometry. *Analytical Biochemistry* **72,** 3573–3580.

Foy DC, Chaney RL, White MC 1978. The physiology of metal toxicity in plants. *Annual Review of Plant Physiology* **29,** 511–566.

Führs H, Hartwig M, Molina LEB, Heintz D, Van Doresslaer A, Braun H-P, Horst WJ 2008. Early manganese-toxicity response in *Vigna unguiculata* L.—a proteomic and transcriptomic study. *Proteomics* **8,** 149–159.

Führs H, Götze S, Specht A, Erban A, Gallien S, Heintz D, Van Dorsselaer A, Kopka J, Braun H-P, Horst WJ 2009. Characterization of leaf apoplastic peroxidases and metabolites in *Vigna unguiculata* in response to toxic manganese supply and silicon. *Journal of Experimental Botany* **60,** 1663–1678.

Führs H, Behrens C, Gallien S, Heintz H, Van Dorsselaer A, Braun H-P, Horst WJ 2010. Physiological and proteomic characterization of manganese sensitivity and tolerance in rice (*Oryza sativa*) in comparison with barley (*Hordeum vulgare*). *Annals of Botany* **105,** 1129–1140.

Herrmann KM, Weaver LM 1999. The shikimate pathway. *Annual Review of Plant Physiology* **50,** 473–503.

Hoffmann L, Maury S, Martz F, Geoffroy P, Legrand M 2003. Purification, cloning, and properties of an acyltransferase controlling shikimate and quinate ester intermediates in phenylpropanoid metabolism. *Journal of Biological Chemistry* **1,** 95–103.

Hoffmann L, Besseau S, Geoffroy P, Ritzenthaler C, Meyer D, Lapierre C, Pollet B, Legrand M 2004. Silencing of hydroxycinnamoyl-coenzyme A shikimate/quinate hydroxycinnamoyltransferase affects phenylpropanoid biosynthesis. *The Plant Cell* **16,** 1446–1465.

Horst WJ, Marschner H 1978. Effect of silicon on manganese tolerance of bean plants (*Phaseolus vulgaris* L.). *Plant and Soil* **50,** 287–303.

Horst WJ. 1988. The physiology of Mn toxicity. In: Webb MJ, Nable RO, Graham RD, Hannam RJ, eds. *Manganese in soil and plants,* Dordrecht: Kluwer Academic Publishers, 175–188.

Hummel J, Strehmel N, Selbig J, Walther D, Kopka J 2010. Decision tree supported substructure prediction of metabolites from GC-MS profiles. *Metabolomics* **6,** 322–333.

Iwasaki K, Maier P, Fecht M, Horst WJ 2002*a*. Effects of silicon supply on apoplastic manganese concentrations in leaves and their relation to manganese tolerance in cowpea (*Vigna unguiculata* (L.) Walp.). *Plant and Soil* **238,** 281–288.

Iwasaki K, Maier P, Fecht M, Horst WJ 2002*b*. Leaf apoplastic silicon enhances manganese tolerance of cowpea (*Vigna unguiculata*). *Journal of Plant Physiology* **159,** 167–173.

Kruse O 2001. Light-induced short-term adaption mechanisms under redox control in the PSII–LHCII supercomplex: LHCII state transitions and PSII repair cycle. *Naturwissenschaften* **88,** 284–292.

Luedemann A, Strassburg K, Erban A, Kopka J 2008. TagFinder for the quantitative analysis of gas chromatography–mass spectrometry (GC-MS) based metabolite profiling experiments. *Bioinformatics* **24,** 732–737.

Maier P 1997. Bedeutung der Kompartimentierung von Mangan und organischen Säuren für die Mangantoleranz von cowpea *(Vigna unguiculata* (L.) Walp.). Ph.D thesis, University of Hannover, Germany, 27–46.

Nable RO, Houtz RL, Cheniae GM 1988. Early inhibition of photosynthesis during development of Mn toxicity in tobacco. *Plant Physiology* **86,** 1136–1142.

Nishizawa A, Yabuta Y, Shigeoka S 2008. Galactinol and raffinose constitute a novel function to protect plants from oxidative damage. *Plant Physiology* **147,** 1251–1263.

Pittman JK 2005. Managing the manganese: molecular mechanisms of manganese transport and homeostasis. *New Phytologist* **167,** 733–742.

Podgornik H, Stegu M, Podgornik A, Perdih A 2001. Isolation and characterization of Mn(III) tartrate from *Phanerochaete chrysosporium* culture broth. *FEMS Microbiology Letters* **201,** 265–269.

Rogalla H and Römheld V 2002. Role of leaf apoplast in silicon-mediated manganese tolerance of *Cucumis sativus L. Plant, Cell and Environment* **25,** 549–555.

Roessner U, Wagner C, Kopka J, Trethewey RN, Willmitzer L 2000. Simultaneous analysis of metabolites in potato tuber by gas chromatography–mass spectrometry. *The Plant Journal* **23,** 131–142.

Saeed AI, Sharov V, White J, *et al*. 2003 TM4: a free, open-source system for microarray data management and analysis. *Biotechniques* **34,** 374–378.

Sanchez DH, Szymanski J, Erban A, Udvardi MK, Kopka J 2010. Mining for robust transcriptional and metabolic responses to long-term salt stress: a case study on the model legume *Lotus japonicus. Plant, Cell and Environment* **33,** 468–480.

Sanchez DH, Pieckenstain FL, Szymanski J, Erban A, Bromke M, Hannah MA, Kraemer U, Kopka J, Udvardi MK 2011. Comparative functional genomics of salt stress in related model and cultivated plants identifies and overcomes limitations to translational genomics. *PLoS ONE* **6,** e17094.

Schauer N, Fernie AR 2006. Plant metabolomics: towards biological function and mechanism. *Trends in Plant Science* **11,** 508–516.

Scholz M, Kaplan F, Guy CL, Kopka J, Selbig J 2005. Non-linear PCA: a missing data approach. *Bioinformatics* **21,** 3887–3895.

Sheveleva E, Chmara W, Bohnert HJ, Jensen RG 1997. Increased salt and drought tolerance by d-ononitol production in transgenic *Nicotiana tabacum* L. *Plant Physiology* **115,** 1211–1219.

Strehmel N, Hummel J, Erban A, Strassburg K, Kopka J 2008. Retention index thresholds for compound matching in GC-MS metabolite profiling. *Journal of Chromatography B* **871,** 182–190.

Walther D, Strassburg K, Durek P, Kopka J 2010. Metabolic pathway relationships revealed by an integrative analysis of the transcriptional and metabolic temperature stress-response dynamics in yeast. *OMICS* **14,** 261–274.

Wariishi H, Valli K, Gold MH 1992. Manganese(II) oxidation by manganese peroxidase from the basidiomycete *Phanerochaete chrysosporium. Journal of Biological Chemistry* **267,** 23688–23695.

Wissemeier AH, Horst WJ 1992. Effect of high light intensity on manganese toxicity symptoms and callose formation in cowpea (*Vigna unguiculata* (L.) Walp.). *Plant and Soil* **143,** 299–309.